Applied Catalysis A: General 502 (2015) 71–77

Contents lists available at ScienceDirect

Applied Catalysis A: General

journal homepage: www.elsevier.com/locate/apcata

Oxidative dehydrogenation of isobutane catalyzed by an activated carbon fiber cloth exposed to supercritical fluids

Nicolas Martin-Sanchez[a], O.S.G.P. Soares[b], Manuel F.R. Pereira[b], M.Jesus Sanchez-Montero[a], José L. Figueiredo[b,*], Francisco Salvador[a]

[a] Departamento de Química-Física, Facultad de Ciencias Químicas, Universidad de Salamanca, Plaza de la Merced s/n, 37008-Salamanca, España
[b] Laboratory of Catalysis and Materials - Associate Laboratory LSRE/LCM, Faculty of Engineering, University of Porto, rua Dr. Roberto Frias, 4200-465 Porto, Portugal

ARTICLE INFO

Article history:
Received 22 April 2015
Received in revised form 29 May 2015
Accepted 31 May 2015
Available online 5 June 2015

Keywords:
Isobutene
Supercritical fluids
Metal-free catalysis
Carbon catalysts
Oxidative dehydrogenation

ABSTRACT

Modifications that supercritical fluids promote in the surface chemistry of carbon materials are scarcely investigated. Due to this lack of knowledge, carbon materials exposed to supercritical fluids have not been tested in any catalytic application. Here, we present the oxidative dehydrogenation of isobutane catalyzed by an activated carbon fiber cloth previously exposed to supercritical carbon dioxide, supercritical water and nitric acid. The role of carbonyl–quinone groups as active sites is confirmed by their direct correlation with catalytic activity. The ability of the active sites to produce isobutene is hindered by the presence of acidic groups. Supercritical treatments develop microporosity, while removing acidic oxygen surface groups and incorporating carbonyl–quinone groups, so they are appropriate methods to develop efficient carbon catalysts for this reaction. Coke deposits formed during reaction modify the surface chemistry and porosity of the catalysts. Samples presenting high surface areas are deactivated by coke deposition more slowly. Thanks to it, fibers exposed to supercritical water showed the best performance.

1. Introduction

Isobutene is widely employed in the chemical industry. Among other applications, isobutene is used in the production of methyl *tert*-butyl ether (MTBE) and ethyl *tert*-butyl ether (ETBE), two additives that enhance the fuel octane number. It is also used as reagent in several polymerization reactions to produce synthetic rubber, antioxidants and various plastics [1]. The oxidative dehydrogenation of isobutane is an alternative production method that overcomes the thermodynamic limitations and high energy requirements of the conventional dehydrogenation route. The oxidative dehydrogenation of isobutane is usually catalyzed by metal oxides [2–5]. However, different carbon materials, such as activated carbons (ACs) [6,7], carbon xerogels [8] or graphitic carbons [9–11], have emerged as alternative metal-free catalysts capable of producing isobutene.

This reaction is explained in terms of a mechanism involving the quinone-hydroquinone redox cycle, as proposed for other hydrocarbons [2,12–14]. Electron-rich quinone groups abstract hydrogen atoms from C—H bonds in the alkane. Then, the corresponding alkene is produced, while the quinone groups are converted into inactive hydroquinone groups. Finally, oxygen acts as a regenerating agent and reacts with hydroquinone groups to re-establish the original quinone groups. On the other hand, coke formation may occur during the reaction. In such cases, coke blocks the porosity and surface oxygen groups of the original catalysts, and the reaction then proceeds on new oxygen groups formed onto the carbonaceous deposits. In conclusion, coke itself finally becomes the true catalyst for the reaction [6,12,14].

This reaction mechanism involves quinone groups as the active sites for oxidative dehydrogenation. As a result, different attempts to tailor the surface chemistry of raw carbon materials have been investigated in order to optimize the catalytic performance; doping with heteroatoms, and exposure to low-temperature oxidizing solutions (nitric acid, hydrogen peroxide) and high-temperature oxidizing (O_2, N_2O), reducing (H_2) or inert (Ar, N_2) gases are some of them [6–9,12].

A yet unexplored method to modify the chemical properties of carbon materials is their exposure to supercritical fluids. Flu-

* Corresponding author. Tel.: +351 22 508 1663; fax: +351 22 508 1449.
E-mail addresses: nicolas_martin@usal.es (N. Martin-Sanchez), salome.soares@fe.up.pt (O.S.G.P. Soares), fpereira@fe.up.pt (M.F.R. Pereira), chusan@usal.es (M.Jesus Sanchez-Montero), jlfig@fe.up.pt (J.L. Figueiredo), salvador@usal.es (F. Salvador).

http://dx.doi.org/10.1016/j.apcata.2015.05.037
0926-860X/

ids heated up and pressurized over their critical constants acquire outstanding properties. Thanks to its mild critical pressure and temperature (P_c = 73.9 bar; T_c = 31 °C), supercritical carbon dioxide ($SCCO_2$) is the most widely used supercritical fluid. Supercritical water (SCW) requires more severe conditions (P_c = 221 bar; T_c = 374 °C), but this fluid is especially interesting due to its high density and diffusivity and its ability to form clusters or to dissolve gases and organic molecules. When both fluids are heated up to an appropriate temperature, they are able to gasify carbon structures; this gasification ability has been used to prepare carbon-based adsorbents [15–19], among other applications. The reports concerning this topic are focused on the development of porosity, but scarce attention is paid to the chemical properties of the materials [20,21].

In this work, we report for the first time not only textural but also chemical modifications suffered by a porous carbon material upon exposure to $SCCO_2$ and SCW. The raw material investigated is an activated carbon fiber (ACF) cloth. The ability of the fibers treated under supercritical conditions to catalyze such an important reaction as the oxidative dehydrogenation of isobutane is investigated. The performance of an ACF exposed to nitric acid is also reported. Characterization of the catalytic activity and determination of possible relationships between the type of modification and the production of isobutene are presented. Indeed, as far as we know, no previous work delves into the catalytic ability of carbon materials exposed to supercritical fluids.

2. Experimental

2.1. Preparation of the catalysts

A commercial ACF cloth supplied by Kynol was used as raw material. This ACF was prepared from the textile fiber Novoloid. This carbon fiber was transformed into ACF by a one-step process combining both carbonization and activation. This step is carried out simply by exposing the textile structures to the products of combustion of natural or liquefied petroleum gas at 900–1000 °C. The as-received material is referred as Original. The fresh cloth was subsequently exposed to different treatments.

Treatments with supercritical fluids were carried out inside a tubular reactor made of Hastelloy. A fixed bed of approximately 5 g of fresh cloth was introduced in the reactor. The maximum temperature of the oven was 700 °C. The reactor was heated to the desired temperature and then it was exposed to a flow of the corresponding supercritical fluid during 180 min. Water purified with a Milli-Q device at ambient temperature, or liquefied CO_2 at −5 °C, were pumped at 3 $cm^3\,min^{-1}$ by means of high pressure pumps. Different treatments at two different temperatures were performed with each supercritical fluid. Samples SCW.500 and SCW.650 were obtained by exposure of the cloth to a SCW flow at 290 bar and 500 or 650 °C, respectively. Samples $SCCO_2$.250 and $SCCO_2$.700 were obtained by exposure of the cloth to a $SCCO_2$ flow at 100 bar and 250 or 700 °C, respectively. Further details concerning the experimental apparatus employed in supercritical treatments can be found elsewhere [22].

The as-received fiber was also subjected to an acidic treatment. A sample modified with HNO_3 was prepared by exposing 5 g of fresh cloth to a boiling 1 M nitric acid solution in a Soxhlet during 180 min. Afterwards the cloth was repeatedly washed with deionized water until any remaining acid was removed.

2.2. Characterization of the catalysts

The textural characterization of the catalysts was based on their N_2 adsorption-desorption and CO_2 adsorption isotherms. N_2 isotherms were determined at −196 °C in a Quantachrome Instruments NOVA 4200e. CO_2 isotherms were determined at 0 °C in a Quantachrome Instruments Autosorb-iQ-MP. Prior to analysis, each sample (0.08–0.1 g) was outgassed under high vacuum at 150 °C overnight. These isotherms were used to calculate the BET surface area (S_{BET}), the micropore volumes determined by N_2 ($V_0(N_2)$) and CO_2 ($V_0(CO_2)$) and the mesopore (V_{meso}) volume.

XPS measurements were made with a VG Scientific ESCALAB 200A spectrometer equipped with a Mg Kα X-ray source, and SEM images were taken using a FEI Quanta 400 FEG ESEM (15 keV) electron microscope. Both analyses were made at the Materials Center of University of Porto (CEMUP).

Thermogravimetric (TG) analysis was performed using a STA 490 PC/4/H Luxx Netzsch thermal analyzer, by heating the sample in helium flow from 50 to 900 °C with a heating rate of 10 °C min^{-1}.

Temperature programmed desorption (TPD) profiles were obtained in an Altamira Instruments AMI-300 apparatus connected to a Dycor Dimaxion Mass Spectrometer. The samples (0.1 g) were placed in a U-shaped quartz tube inside an electrical furnace and heated at 5 °C min^{-1} from room temperature to 1100 °C under a constant flow rate of helium (25 $cm^3\,min^{-1}$). The amounts of CO and CO_2 released were monitored and the obtained TPD profiles were deconvoluted in order to identify and quantify the surface oxygen groups [23,24]. All the TPD spectra are shown in the Supplementary data.

2.3. Catalytic tests

The catalytic tests were performed by packing several round-shaped layers of the cloth (0.2 g) inside a stainless steel tubular reactor (Microactivity Reference, PID Eng & Tech). Mass flow controllers were used to set the gas flow rates. The reaction mixture was obtained by mixing 4 $cm^3\,min^{-1}$ isobutane, 2 $cm^3\,min^{-1}$ O_2 and 24 $cm^3\,min^{-1}$ N_2. The reaction temperature, 375 °C, was measured by a thermocouple and maintained throughout the 300 min of reaction. The gaseous products of the reaction were analyzed by a GC 1000 Dani chromatograph equipped with a Chrompack Capilary Column CP Sil 8CB low bleed/ms 30 m × 0.32 mm, 1 μm, and an online non-dispersive infrared (NDIR) analyzer for CO_2.

The catalyst performance was evaluated in terms of the following parameters:

$$\text{Conversion} \quad X_{\text{isobutane, inlet (\%)}} = \frac{F_{\text{isobutane, inlet}} - F_{\text{isobutane, outlet}}}{F_{\text{isobutane, inlet}}} \times 100$$

$$\text{Isobutene yield} \quad R_{\text{isobutene}}(\%) = \frac{F_{\text{isobutene,outlet}}}{F_{\text{isobutane,inlet}}} \times 100$$

$$\text{Isobutene selectivity}\, S_{\text{isobutene}}(\%) = \frac{F_{\text{isobutene,outlet}}}{F_{\text{isobutene,inlet}} - F_{\text{isobutene, outlet}}} \times 100$$

$$CO_2 \text{ selectivity}\, S_{CO2}(\%) = \frac{F_{CO2,\text{outlet}/4}}{F_{\text{isobutane,inlet}} - F_{\text{isobutane,outlet}}} \times 100$$

Where X is the conversion, F is the molar flow rate, R is the yield and S is the selectivity.

3. Results

3.1. Characterization of the catalysts

Table 1 shows the textural properties of the original and modified fibers. The raw material is essentially microporous, as reflected by its high S_{BET} and micropore volumes (Table 1). Nitric acid partially destroys the microporosity due to its strong acidic character. The micropore volume decreases while the mesoporosity and the

Table 1
Textural characterization of Original and modified fibers.

Sample	S_{BET}($m^2\ g^{-1}$)	$V_0(N_2)$($cm^3\ g^{-1}$)	V_{meso}($cm^3\ g^{-1}$)	$V_0(CO_2)$($cm^3\ g^{-1}$)
Original	1030	0.511	0.008	0.397
HNO_3-modified	1078	0.439	0.012	0.359
SCW.500	1356	0.554	0.006	0.382
SCW.650	1438	0.590	0.002	0.341
$SCCO_2$.250	1112	0.524	0.002	0.383
$SCCO_2$.700	1300	0.540	0.001	0.384

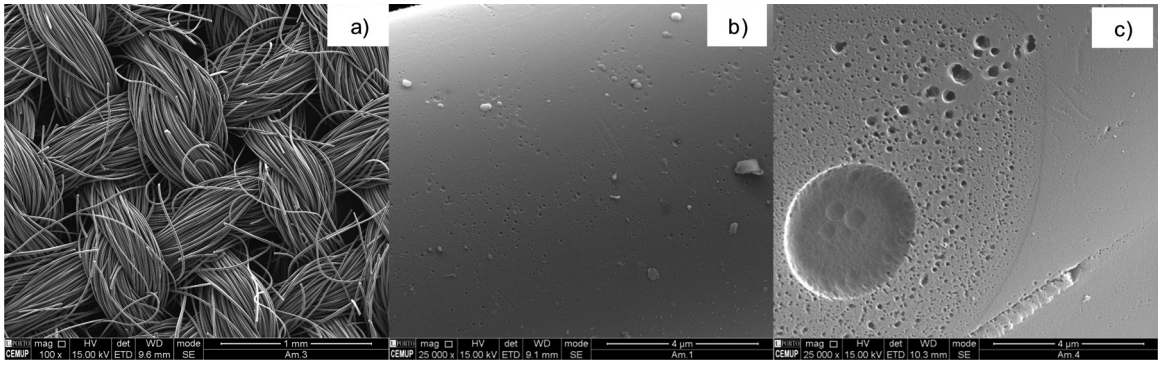

Fig. 1. SEM images of the Original fibers (a and b) and the fibers modified with HNO_3 (c).

Table 2
XPS analysis of the Original and modified fibers.

Sample	C (wt.%)	N (wt.%)	O (wt.%)
Original	93.3	0.74	5.95
HNO_3-modified	80.2	1.07	18.7
SCW.500	95.8	0.09	4.11
SCW.650	97.7	0.10	2.23
$SCCO_2$.250	92.7	0.32	6.98
$SCCO_2$.700	95.7	0.07	4.21

available surface area slightly increase. Fig. 1, where SEM images of Original fibers and of the fibers modified with HNO_3 are presented, highlights the aggressiveness of this treatment.

The exposure of the cloth to both supercritical fluids also changes its textural characteristics. In previous works, it was checked that SCW gasifies this material at temperatures higher than 600 °C [22]. In order to analyze the influence of gasification on the catalytic performance of the fibers, treatments below and above this temperature were carried out. Although SCW.500 is not gasified, some pore opening occurs, thus resulting in higher S_{BET} and $V_0(N_2)$. SCW.650 does suffer gasification. Specifically, a mass loss of about 15% was measured after 3 h of treatment. Gasification of the carbon structure of SCW.650 fiber exerts a similar effect on the textural properties as in the previous case, but pore widening and development of the surface area are more marked. Consequently, both samples exposed to SCW have a more developed microporosity than Original.

Sample $SCCO_2$.250 is treated under conditions at which gasification does not take place. In spite of this, $SCCO_2$ at 250 °C is also able to unblock a few pore entrances. Surface area increases to a small extent because some micropores become accessible. We also wanted to evaluate the importance of gasification with $SCCO_2$, but this fluid is a less reactive gasifying agent than SCW, so higher temperatures had to be employed. The raw material was gasified by a $SCCO_2$ stream heated up at 700 °C and it lost about 8% of mass after 3 h. Some of the inaccessible pores became available and new micropores appeared, as reflected by the increase of S_{BET} and $V_0(N_2)$.

XPS analysis was performed for all the samples. Table 2 reveals that the acidic and supercritical treatments not only modify the textural properties but also the chemical surface composition of the raw material. Nitric acid incorporates large amounts of oxygen and small amounts of nitrogen onto the carbon structure. The fibers treated with supercritical fluids have lower oxygen contents than Original, except $SCCO_2$.250, whose oxygen content increases from 5.95% to 6.98%.

TPD analysis was also performed in order to assess eventual changes in the oxygen-containing surface groups. The oxygenated groups decompose by releasing CO_2 (carboxylic acids, anhydrides, lactones) or CO (anhydrides, phenols, carbonyl–quinones) at different temperatures. The TPD profiles were deconvoluted according to the methodology described elsewhere [23,24], and the results are shown in Table 3.

As suggested by XPS analysis, large amounts of oxygen surface groups are incorporated upon treatment with nitric acid, significant amounts of CO_2 and CO being released by the sample modified with HNO_3. SCW.500 and SCW.650 present no carboxylic acid, anhydride and lactone groups, and only a small amount of phenol groups due to the high temperatures required in the supercritical treatments with this fluid. The temperatures used in the supercritical treatments have removed the carboxylic acid and anhydride groups since they are released at temperatures below 450 °C and 650 °C, respectively [23]. Phenol groups were partially removed since they are decomposed in the range 550–700 °C. On the contrary, there is an increase in the number of carbonyl–quinone groups close to 25%, since these groups are only released as CO in the range 700–950 °C, which is higher than the temperature used in the supercritical treatments. The low critical temperature of CO_2 allows milder treatments to be realized. For that reason, $SCCO_2$.250 preserves some carboxylic acid groups, since they are released at temperatures between 200 and 450 °C. Regarding the other groups, large amounts of them remain after the supercritical treatment. This is especially marked for phenol groups, since their content rises from 464 $\mu mol\ g^{-1}$ to 926 $\mu mol\ g^{-1}$. The severe conditions employed in the preparation of $SCCO_2$.700 remove from the carbon surface all the carboxylic acid, anhydride and lactone groups and a third of the phenols. As in the other samples exposed to supercritical fluids, the modified material has more carbonyl–quinone groups than the Original sample, the samples treated with CO_2 being those with the highest amount of this group.

Table 3
Results of the deconvolution of TPD spectra of Original and modified fibers.

Sample	Carboxylic acid(±20 μmol/g)	Anhydride(±20 μmol/g)	Lactone(±20 μmol/g)	Phenol(±20 μmol/g)	Carbonyl-quinone(±20 μmol/g)
Original	316	149	63	464	744
HNO_3-modified	3654	978	459	2599	3282
SCW.500	–	–	–	108	927
SCW.650	–	–	–	156	942
$SCCO_2$.250	111	206	77	926	1068
$SCCO_2$.700	–	–	–	289	1025

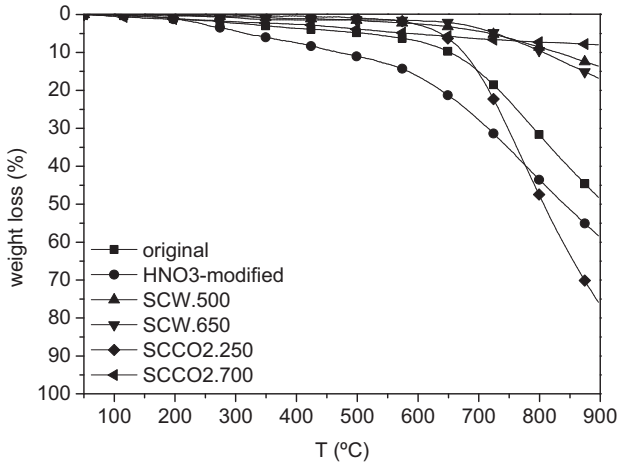

Fig. 2. TGA profiles of original and modified fibers.

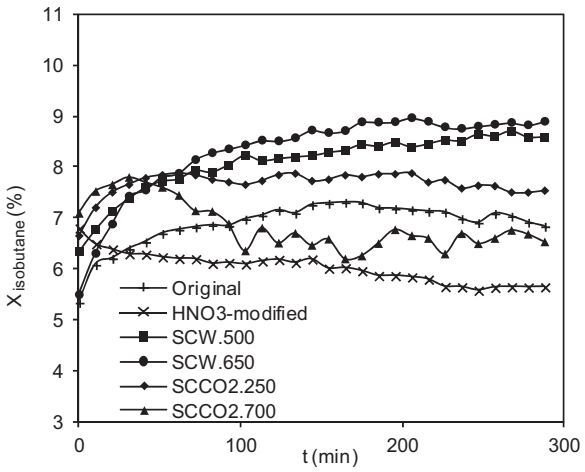

Fig. 3. Conversion of isobutane as a function of reaction time with Original and modified catalysts.

Thermogravimetric analyses (TGA) were performed for all the samples and Fig. 2 shows their TGA profiles. Samples treated at high supercritical temperatures present the highest thermal stability. Significant weight loss is observed for Original, modified with HNO_3 and $SCCO_2$.250 samples (48, 58 and 76 %, respectively), which is related to the high amount of oxygenated surface groups of these samples (determined by TPD) that are released during heating, and also with the pyrolysis of the compounds present in the Original fiber, whose one-step activation process does not assure the complete removal of all the volatile compounds that it contains. The decomposition of the sample modified with HNO_3 starts at lower temperatures compared to the other samples, due to the large amount of carboxylic acids present in this sample.

XPS, TPD and TGA analyses provide new information about the interaction between carbon materials and supercritical fluids. SCW and $SCCO_2$ modify the surface chemistry of carbon materials irrespective of gasification occurring or not. Under the experimental conditions here employed, $SCCO_2$ introduces more oxygen surface groups than SCW, although extrapolation of this conclusion to unexplored pressures or temperatures might be risky. Differences caused by gasification are clearer for $SCCO_2$ because SCW's critical temperature is very high. Hotter and/or longer treatments with SCW would emphasize the influence of gasification on surface chemistry.

The data presented here display important changes in the surface chemistry caused by gasification. As expected, the high temperatures used decompose the less stable groups, like carboxylic acids or anhydrides; however, a concomitant and unexpected increase of carbonyl–quinone groups is measured. In summary, the nature and the amount of oxygen surface groups are modified during gasification, therefore they may play an important role in this process. These results had not been observed previously and may provide relevant information about the development of supercritical gasification since, despite the research concerning C/H_2O and C/CO_2 reactions under supercritical conditions, the true pathways involved in these reactions remain uncertain to date [17–19,22,25].

3.2. Catalytic performance of the ACFs

Catalytic performance of the fibers for the oxidative dehydrogenation of isobutane as a function of the reaction time will be analyzed in terms of the effect of the different treatments. The conversion of isobutane obtained with the different catalysts is reported in Fig. 3.

This figure shows different performances depending on the catalyst employed. The initial isobutane conversion obtained with Original catalyst is the lowest, but during the initial stages of the reaction there is a clear increase after which it remains practically constant. $SCCO_2$.250 performs in a similar way, although it is able to convert more isobutane than Original. The conversion profile achieved by $SCCO_2$.700 is different. There is also an initial increase in conversion, but in this case it is followed by a noticeable decrease. After that, the conversion remains almost constant (or slightly decreases). SCW.500 and SCW.650 present the best performances. In the earliest moments of the reaction, the other catalysts convert more isobutane than them; however, their corresponding conversions increase during the whole reaction (after 5 h they do not reach the plateau observed for Original and $SCCO_2$.250 catalysts), in such a way that they finally convert the largest amounts of isobutane. The catalyst exposed to HNO_3 behaves differently than the other ACFs. The acidic fibers exhibit the lowest isobutane conversion and, moreover, the conversion profile decreases continuously with time on stream.

Fig. 4a shows the selectivities to CO_2 and isobutene. Only the use of catalysts exposed to $SCCO_2$ promotes the formation of CO_2, although selectivities just above 5% are obtained. Blank experiments without isobutane feeding were carried out and no CO_2 was measured, confirming that this CO_2 does proceed from the reaction. Fig. 4a also reveals that different samples do not lead to appreciable differences in the isobutene selectivities. All of them remain essentially constant with time and range from 91 to 95% during the reaction. These selectivities are lower than 100% due to the forma-

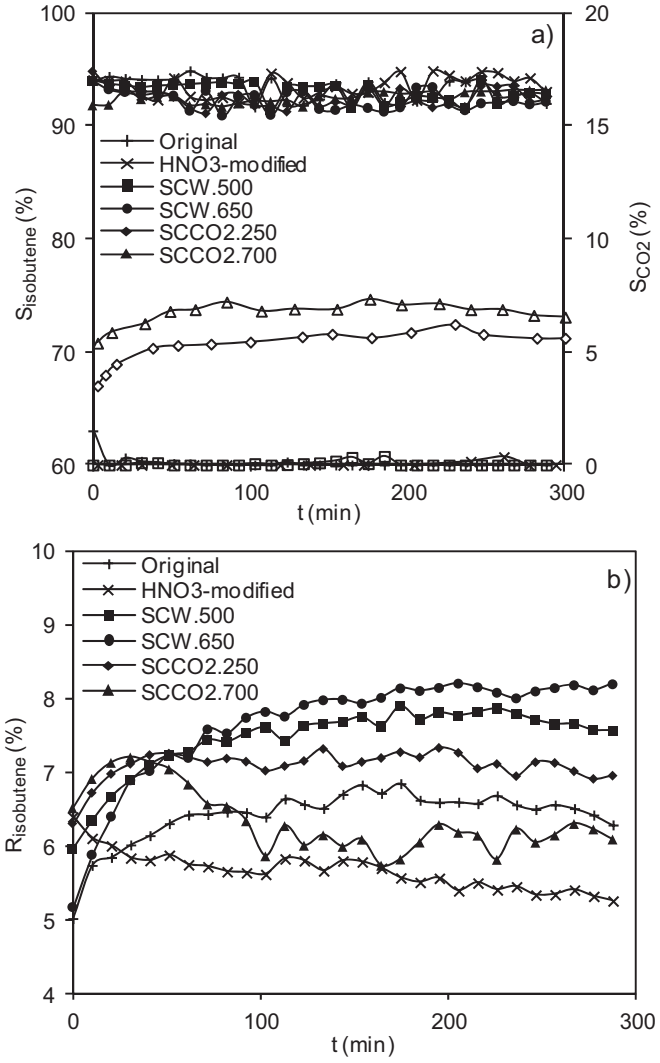

Fig. 4. (a) Isobutene selectivity (filled symbols) and CO_2 selectivity (open symbols) as a function of reaction time with Original and modified catalysts. (b) Isobutene yield as a function of reaction time with Original and modified catalysts.

tion of coke, CO_2 and some unidentified gaseous products detected in the GC analysis. Blank experiments were performed to confirm that these products (up to four products different from isobutene were detected) came from the reaction and not from the eventual decomposition of the catalysts.

The obtained selectivities originate isobutene yield profiles (Fig. 4b) which are similar to those previously described for isobutane conversion. As a result, the amount of isobutene formed strongly depends on the sample. Catalyst SCW.650 is especially interesting. It leads to the highest yield, which is still increasing after 5 h, thus suggesting that it should be able to catalyze this reaction during longer periods of time without a significant loss of activity. The other catalysts produce lower isobutene amounts. Moreover, at the end of the reaction their yields reach a plateau or decrease slightly, this last trend reflecting that the catalysts begin to deactivate.

It is well-known that carbonyl–quinone groups are the active sites for the oxidative dehydrogenation of isobutane and other hydrocarbons [2,6,12,14]. Then, at the initial moments of the reaction, the isobutene yield should be directly determined by the number of these oxygen groups present on the surface of the fresh catalysts. The data shown in Fig. 5 supports this argument.

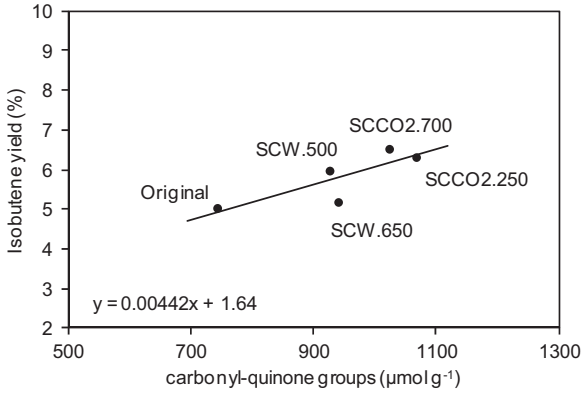

Fig. 5. Correlation between the isobutene yield measured at the beginning of the reaction and the initial concentration of carbonyl–quinone groups on the surface of Original and modified catalysts.

Considering just the active sites is essential to obtain a correct correlation. When all oxygen groups are considered, no coherent correlation is observed [26,27]. A positive intercept indicates that active sites are introduced onto the catalyst surface by oxygen present on the reaction mixture. The low conversions achieved allow assuming a differential reactor behavior; accordingly, the turn-over frequency (TOF) for the oxidative dehydrogenation of isobutane under these conditions can be calculated as follows:

$$\text{TOF} = \frac{s \times F_{\text{isobutane,inlet}}}{m} = 6.03 \times 10^{-4} \mu\text{mol}_{\text{isobutene}}\, \mu\text{mol}_{\text{carbonyl-quinone}}{}^{-1} s^{-1}$$

where s is the slope of the correlation in Fig. 5 and m is the catalyst mass used, 0.2 g.

Scarce TOF data of metal-free carbon catalysts for this reaction have been reported. There is only one work [8], where oxidized carbon xerogels treated at different temperatures under inert atmosphere are tested, reporting an initial TOF of 3.17×10^{-4} $\mu\text{mol}_{\text{isobutene}}$ $\mu\text{mol}_{\text{carbonyl-quinone}}{}^{-1}$ s^{-1} measured at the same conditions investigated in the present work.

It must be remarked that the sample modified with HNO_3 does not appear in Fig. 5 because it does not fit the correlation. This catalyst leads to an initial yield of 6.4%, which clearly disagrees with its initial carbonyl–quinone concentration, 3282 $\mu\text{mol g}^{-1}$. This is caused by the great abundance of anhydride groups on the carbon surface. This sample also contains large amounts of carboxylic acid groups, but these will be decomposed at the reaction temperature. Acidic groups tend to decrease the electron density at the active sites, thus reducing their catalytic activity [8]. The acidic character of the catalyst previously exposed to HNO_3 explains its poor ability to dehydrogenate isobutane reflected in Figs. 3 and 4b. Consequently, isobutene yields are lower than expected when the concentration of active sites is considered. Original and $SCCO_2$.250 samples contain a few of these acidic groups but, in contrast to the sample modified with HNO_3, their performances fit the general correlation due to their mild acidic character.

In summary, it can be stated that efficient carbon catalysts for the oxidative dehydrogenation of isobutane can be obtained by exposure of ACFs to supercritical fluids. SCW and $SCCO_2$ are able to remove acidic groups that reduce the catalytic activity and promote the formation of carbonyl–quinone groups, which act as active sites.

3.3. Coke formation and its effect on catalytic performance

The development of the reaction at the beginning mainly depends on the characteristics of the fresh catalysts, but they suffer modifications throughout the reaction that strongly affect their performances [6,14]. Firstly, coke deposits are formed, blocking the porosity of the catalysts. Secondly, oxygen in the feed is capable

Table 4
Changes in textural properties of the catalysts after reaction.

Sample	ΔS_{BET}(%)	$\Delta V_0(N_2)$(%)	ΔV_{meso}(%)	$\Delta V_0(CO_2)$(%)
Original	−21.5	−35.2	+175	−42.1
HNO_3-modified	−41.5	−39.6	+58	−50.1
SCW.500	−39.6	−39.2	+167	−47.9
SCW.650	−35.7	−35.6	+250	−42.2
$SCCO_2$.250	−47.6	−47.5	+650	−48.0
$SCCO_2$.700	−55.9	−55.0	+1500	−44.3

of introducing active sites onto the carbon surface at the reaction temperature. Both changes can be evaluated by analyzing the catalysts after being used in the dehydrogenation of isobutane. Coke formation was evaluated by textural characterization and TG.

Table 4 reports the changes in textural properties after dehydrogenation. Blockage of porosity caused by coke formation is evident, with a considerable decrease of surface area and micropore volumes. Mesoporosity appears to suffer a large increase, but these numerical data are originated by the extremely low V_{meso} values of the fresh catalysts; all the catalysts remaining essentially microporous. According to Table 4, the available surface area decreases as reaction proceeds, whereas yield goes up or stabilizes (Fig. 4). This opposite behavior clearly demonstrates that surface area plays no direct role in the catalytic performance [26]. Textural characterization after reaction also reveals that these catalysts preserve 45–80% of their initial surface area despite coke deposition after 5 h. Similar reductions were found in a microporous commercial AC for the same reaction [6].

Modifications in the surface chemistry by the catalytic process were studied by TPD. Table 5 collects the deconvolution results of the TPD profiles. Higher amounts of CO and CO_2 are released during the TPD analysis after the ODH process. Anhydride, lactone and carbonyl–quinone groups are more abundant, although phenol groups suffer the largest increase. Both the initial porosity and the oxygen surface groups are blocked by coke formation. The presence of oxygen in the reaction mixture forms new groups onto the coke surface, so the coke itself acts as catalyst [6,12,14]. The tendencies of Fig. 4b can be explained according to this fact.

The plateau reached by $SCCO_2$.250 and $SCCO_2$.700 suggests that the number of groups being blocked by coke is similar to the number of groups being formed onto it. Coke blockage in $SCCO_2$ samples is larger than in SCW samples, probably because of the higher S_{BET} and $V_0(N_2)$ of SCW.500 and SCW.650. Then, due to this softer blockage, the original groups being disabled in SCW catalysts may be less numerous than the new groups being formed. This fact would explain that equilibrium is not reached after 5 h and allows the final increasing trend of the yield to be explained.

Fig. 6 shows that the catalysts used in the reaction start to lose weight earlier than the fresh catalysts (Fig. 2), confirming coke formation on the catalysts surface. The exception is the sample exposed to HNO_3, which only starts to lose weight at temperatures higher than the reaction temperature; at the reaction temperature the carboxylic acids and anhydrides are removed from the carbon surface (Table 5).

It can be concluded that treatments with SCW are an especially appropriate method to tailor the properties of carbon catalysts for

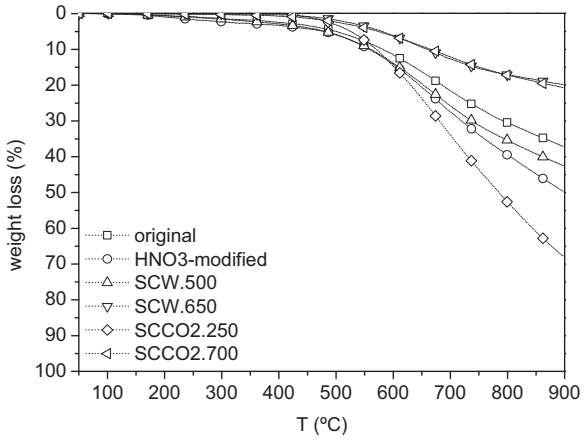

Fig. 6. TGA profiles of original and modified fibers after reaction.

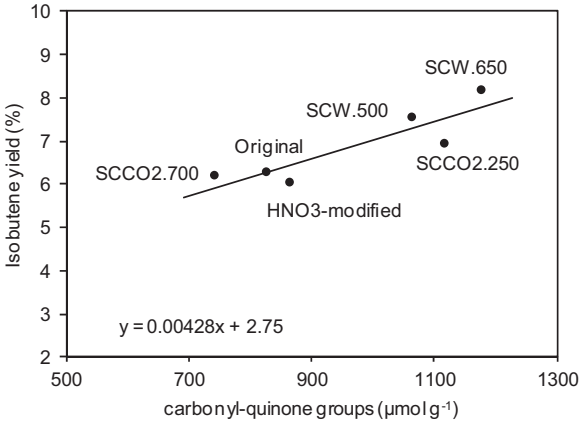

Fig. 7. Correlation between the isobutene yield measured at the end of the reaction and the concentration of carbonyl–quinone groups on the surface of Original and modified catalysts after reaction.

this reaction. On one hand, this supercritical fluid is able to remove harmful acidic groups and to incorporate carbonyl–quinone groups that act as active sites. On the other hand, it develops the surface area which does not affect directly the catalytic ability, but seems to delay the deactivation associated to coke formation.

The characterization of the catalysts surface chemistry at the end of the reaction allows to obtain a relationship between the final catalytic activity and the active sites present after 5 h of reaction. Fig. 7 shows this correlation. These data lead to a final TOF value of 5.83×10^{-4} $\mu mol_{isobutene}$ $\mu mol_{carbonyl\text{-}quinone}^{-1}$ s^{-1}, which is similar to the initial one, although the final yields are higher (except for the catalyst modified with HNO_3) due to the higher amounts of carbonyl–quinone groups of the ACFs at the end of the reaction.

Table 5
Results of the deconvolution of TPD spectra of Original and modified fibers after reaction.

Sample	Carboxylic acid(±20 μmol/g)	Anhydride(±20 μmol/g)	Lactone(±20 μmol/g)	Phenol(±20 μmol/g)	Carbonyl-quinone(±20 μmol/g)
Original	56	270	1332	5748	826
HNO_3-modified	120	480	2496	6372	864
SCW.500	–	300	2688	7204	1063
SCW.650	–	179	2112	11628	1176
$SCCO_2$.250	–	184	1656	5676	1116
$SCCO_2$.700	–	360	2015	6060	742

4. Conclusions

In this work, we present the catalytic performance of a carbon material exposed to supercritical fluids and nitric acid in the oxidative dehydrogenation of isobutane. Modifications in an ACF cloth after exposing it to $SCCO_2$, SCW and nitric acid are presented. Both supercritical fluids and nitric acid modify the textural and surface chemical properties of the raw material. $SCCO_2$ and SCW unblock and develop microporosity, remove acidic oxygen groups and incorporate additional carbonyl-quinone groups. Nitric acid destroys a few micropores and introduces large amounts of oxygen surface groups, especially carboxylic acids.

Carbonyl–quinone groups are confirmed to be the active sites for the reaction, while acidic groups reduce their catalytic activity. This reaction mechanism implies that exposure to supercritical fluids constitutes a suitable method to prepare efficient catalysts for isobutane oxidative dehydrogenation, while nitric acid is not appropriate. Clear evidences for coke formation are reported; it blocks porosity and becomes the true catalyst as reaction proceeds. Despite coke formation, SCW catalysts show the best performance: they lead to selectivities close to 95%, their yields are the highest and their activity profiles still describe an increasing trend at the end.

Acknowledgments

Financial support from the Spanish Ministerio de Economía y Competitividad (Project CTQ2012-30909) and Anticipios Fondos Feder is acknowledged.

LCM group acknowledges projects UID/EQU/50020/2013, co-financed by FCT - Fundação para a Ciência e a Tecnologia and FEDER; and NORTE-07-0162-FEDER-000050 and NORTE-07-0124-FEDER-000015, co-financed by QREN, ON2 and FEDER, under Programe COMPETE. O.S.G.P. Soares acknowledges the grant received from FCT (SFRH/BPD/97689/2013).

Appendix A. Supplementary data

Supplementary data associated with this article can be found, in the online version, at http://dx.doi.org/10.1016/j.apcata.2015.05.037

References

[1] B.N.M. van Leeuwen, A.M. van der Wulp, I. Duijnstee, A.J.A. van Mars, A.J.J. Straathof, Appl. Microbiol. Biotechnol. 93 (2012) 1377–1387.
[2] J. Zhang, D. Su, A. Zhang, D. Wang, R. Schlög, C. Hébert, Angew. Chem. Int. Ed. 46 (2007) 7319–7323.
[3] G. Wang, L. Zhang, J. Deng, H. Dai, H. He, C. Tong-Au, Appl. Catal. A: Gen. 355 (2009) 192–201.
[4] J. Sloczynski, B. Grzybowska, A. Kozlowska, K. Samson, R. Grabowski, A. Kotarba, M. Hermanowska, Catal. Today 169 (2011) 29–35.
[5] G. Wang, H. Dai, L. Zhang, J. Deng, C. Liu, H. He, C. Tong-Au, Appl. Catal. A: Gen. 375 (2010) 272–278.
[6] J.J. Díaz-Velásquez, L.M. Carballo-Suárez, J.L. Figueiredo, Appl. Catal. A: Gen. 311 (2006) 51–57.
[7] I. Gniot, P. Kirszensztejn, M. Kozlowski, Appl. Catal. A: Gen. 362 (2009) 67–74.
[8] I. Pelech, O.S.G.P. Soares, M.F.R. Pereira, J.L. Figueiredo, Catal. Today 249 (2015) 176–183.
[9] V. Schwartz, H. Xie, H.M. Meyer III, S.H. Overbury, C. Liang, Carbon 49 (2011) 659–668.
[10] H. Xie, Z. Wu, H. Steven, C. Liang, V. Schwartz, J. Catal. 267 (2009) 158–166.
[11] G.K.P. Dathar, Y.T. Tsai, K. Gierszal, Y. Xu, C. Liang, A.J. Rondinone, S.H. Overbury, V. Schwartz, Chemsuschem 7 (2014) 483–491.
[12] M.F.R. Pereira, J.J.M. Órfão, J.L. Figueiredo, Appl. Catal. A: Gen. 184 (1999) 153–160.
[13] M.F.R. Pereira, J.J.M. Órfão, J.L. Figueiredo, Appl. Catal. A: Gen. 196 (2000) 43–54.
[14] M.F.R. Pereira, J.J.M. Órfão, J.L. Figueiredo, Appl. Catal. A: Gen. 218 (2001) 307–318.
[15] F. Salvador, M.J. Sánchez Montero, J. Montero, C. Izquierdo, J. Power Sources 190 (2009) 331–335.
[16] J. García-Serna, E. García-Merino, M.J. Cocero, J. Supercrit. Fluids 43 (2007) 228–235.
[17] D. Montané, V. Fierro, J.F. Marêché, L. Aranda, A. Celzard, Micropor. Mesopor. Mat. 119 (2009) 53–59.
[18] J. Montero, M.A. de la Casa-Lillo, M.J. Sanchez-Montero, N. Martin-Sanchez, C. Izquierdo, F. Salvador, J. Supercrit. Fluids 101 (2015) 131–139.
[19] R. Zhang, W. Jiang, L. Cheng, B. Sun, D. Sun, J. Bi, Int. J. Hydrogen Energy 35 (2010) 11810–11815.
[20] J.L. Figueiredo, N. Mahata, M.F.R. Pereira, M.J. Sánchez Montero, J. Montero, F. Salvador, J. Colloid Interface Sci. 357 (2011) 210–214.
[21] A. Ashraf, S.A. Dastgheib, G. Mensing, M.A. Shannon, J. Supercrit. Fluids 76 (2013) 32–40.
[22] N. Martin-Sanchez, F. Salvador, M.J. Sanchez-Montero, C. Izquierdo, J. Phys. Chem. Lett. 5 (2014) 2613–2618.
[23] J.L. Figueiredo, M.F.R. Pereira, M.M.A. Freitas, J.J.M. Órfão, Carbon 37 (1999) 1379–1389.
[24] J.L. Figueiredo, M.F.R. Pereira, M.M.A. Freitas, J.J.M. Órfão, Ind. Eng. Chem. Res. 46 (2007) 4110–4115.
[25] M. Molina-Sabio, M.J. Sánchez-Montero, J.M. Juárez-Galán, F. Salvador, F. Rodríguez-Reinoso, A. Salvador, J. Phys. Chem. B 110 (2006) 12360–12364.
[26] V. Schwartz, W. Fu, Y.T. Tsai, H.M. Meyer III, A.J. Rondinone, J. Chen, Z. Wu, S.H. Overbury, C. Liang, Chemsuschem 6 (2013) 840–846.
[27] C. Liang, H. Xie, V. Schwartz, J. Howe, S. Dai, S.H. Overbury, J. Am. Chem. Soc. 131 (2009) 7735–7741.